filtered into an extraction thimble and then washed by Soxhlet extraction with methanol, hexane, and chloroform. The polymer was isolated from the chloroform extracts. End-group composition was evaluated with MALDI-TOF MS (Voyager-DE STR BioSpectrometry workstation by Biosystems, terthiophene matrix, linear mode, sometimes performed before extractions), and the polymer structure was confirmed with ^{1}H NMR (Bruker 500 MHz instrument).

Received: January 29, 2004
Final version: March 9, 2004

[1] a) J. R. Kline, M. D. McGehee, E. N. Kadnikova, J. Liu, J. M. J. Frechet, *Adv. Mater.* **2003**, *15*, 1519. b) A. R. Brown, C. M. Pomp, D. M. de Leeuw, *Science* **1995**, *270*, 972. c) H. Sirringhaus, P. J. Brown, R. H. Friend, M. M. Nielsen, K. Bechgaard, B. M. W. Langeveld-Voss, A. J. H. Spiering, R. A. J. Janssen, E. W. Meijer, P. Herwig, D. M. de Leeuw, *Nature* **1999**, *401*, 685. d) H. Sirringhaus, N. Tessler, R. H. Friend, *Science* **1998**, *280*, 1741. e) W. U. Huynh, J. J. Dittmer, P. Alivasatos, *Science* **2002**, *295*, 2425. f) Z. Bao, A. Dodabalapur, A. J. Lovinger, *Appl. Phys. Lett.* **1996**, *69*, 3.

[2] a) R. D. McCullough, R. D. Lowe, M. Jayaraman, D. L. Anderson, *J. Org. Chem.* **1993**, *58*, 904. b) T. A. Chen, X. Wu, R. D. Rieke, *J. Am. Chem. Soc.* **1995**, *117*, 233.

[3] R. S. Loewe, S. M. Khersonsky, R. D. McCullough, *Adv. Mater.* **1999**, *11*, 250.

[4] R. D. McCullough, *Adv. Mater.* **1998**, *10*, 93.

[5] J. Liu, R. D. McCullough, *Macromolecules* **2002**, *35*, 8.

[6] a) B. M. W. Langeveld-Voss, R. A. J. Janssen, A. J. H. Spiering, J. L. J. van Dongen, E. C. Vonk, H. A. Claessens, *Chem. Commun.* **2000**, *2000*, 81. b) M. Jayakannan, J. L. J. v. Dongen, R. A. J. Janssen, *Macromolecules* **2001**, *34*, 8. c) A. Iraqi, G. W. Barker, *J. Mater. Chem.* **1998**, *8*, 25.

[7] J. Liu, E. Sheina, T. Kowalewski, R. D. McCullough, *Angew. Chem. Int. Ed.* **2002**, *41*, 4.

[8] E. Sheina, J. Liu, M. C. Iovu, D. W. Laird, R. D. McCullough, *Macromolecules* **2004**, *37*, 3526.

[9] R. S. Loewe, P. C. Ewbank, J. S. Liu, L. Zhai, R. D. McCullough, *Macromolecules* **2001**, *34*, 4324.

[10] J. Liu, R. S. Loewe, R. D. McCullough, *Macromolecules* **1999**, *32*, 5777.

[11] The unsaturated component could be from either the excess Grignard reagent or the mono-capped polymer **3**.

[12] K. Tamao, K. Sumitani, Y. Kiso, M. Zembayashi, A. Fujioka, S.-I. Kodama, I. Nakajima, A. Minato, M. Kumada, *Bull. Chem. Soc. Jpn.* **1976**, *49*, 1958.

[13] a) R. H. Crabtree, *The Organometallic Chemistry of the Transition Metals*, 3rd ed., John Wiley & Sons, New York **2001**. b) C. A. Tolman, W. C. Seidel, L. W. Gosser, *Organometallics* **1983**, *2*, 1391.

[14] M. C. Iovu, E. Sheina, G. Sauvé, M. Jeffries-EL, J. Cooper, R. D. McCullough, *Polym. Prepr. (Am. Chem. Soc., Div. Polym. Chem)* **2004**, *45*, 278.

[15] Characterization of (H/Br poly(3-hexylthiophene): ^{1}H NMR (500 MHz, $CDCl_3$): δ_H 0.91 (t, J = 7 Hz, 3H), 1.40 (m, 6H), 1.69 (t, J = 7 Hz, 2H), 2.80 (t, J = 7 Hz, 2H), 7.46 (s, 1H); GPC: M_n: 11 364, PDI: 1.2; MALDI-MS: m/z: 6239.4 [M$^+$] (calcd: 6231.2, DP of 46, H/Br end groups). Characterization of **1**: ^{1}H NMR (500 MHz, $CDCl_3$): Hexyl peaks are the same as above with δ_H 5.11 (d, J = 11 Hz, 1H), 5.49(d, J = 11 Hz, 1H), 6.20 (m, 1H), 7.14 (s, 55H); GPC: M_n: 11 218, PDI: 1.1; MALDI-MS: m/z: 4927.2 [M$^+$] (calcd: 4927.7, DP of 29, Br/Vinyl end groups). Characterization of **2**: ^{1}H NMR (500 MHz, $CDCl_3$): Hexyl peaks same as above with δ_H 3.49 (d, J = 6.5 Hz, 2H), 5.12 (d, J = 6.5 Hz, 2H), 5.98 (m, 1H), 7.14 (s, 44H); GPC: M_n: 6068, PDI: 1.1; MALDI-MS: m/z: 4110.3 [M$^+$] (calcd: 4111.6, DP of 24, Br/Allyl end groups). Characterization of **10** (uncapped): ^{1}H NMR (500 MHz, THF d_8): δ_H 0.92 (t, J = 7 Hz, 3H), 1.37 (m, 6H), 2.85 (t, J = 7 Hz, 2H), 7.08 (s, 1H), (remaining two protons buried under solvent peak); GPC: M_n: 11 200, PDI: 1.2; MALDI-MS: m/z: 7561.0 [M$^+$] (calcd: 7561.4, DP of 45, H/Br end groups). Characterization of **3**: ^{1}H NMR (500 MHz, THF d_8): (Hexyl peaks are the same as for **10** with, δ_H 4.12 (s, 1H), 7.05 (s, 39H); GPC: M_n: 8232, PDI: 1.4; MALDI-MS: m/z: 5768.0 [M$^+$] (calcd: 5758.6, DP of 34, ethynyl/Br end groups). Characterization of **4**: ^{1}H NMR (500 MHz, THF d_8): (Hexyl peaks same as for **10** with, δ_H 7.11 (s, 41H), 7.43 (m, 2H), 7.47 (m, 8H); GPC: M_n: 12 000, PDI: 1.1; MALDI-MS: m/z: 8305.9 [M$^+$] (calcd: 8302.2, DP of 49, phenyl/phenyl endgroups). Characterization of **5**: ^{1}H NMR (500 MHz, THF d_8): (Hexyl peaks same as for **10** with, δ_H 7.10 (s, 29H), 7.24 (d, J = 8 Hz, 4H), 7.36(d, J = 8 Hz, 4H); GPC: M_n: 6700, PDI: 1.1; MALDI-MS: m/z: 4508.6 [M$^+$] (calcd: 4505.6, DP of 26, tolyl/tolyl). Characterization of **6**: ^{1}H NMR (500 MHz, THF d_8): (Hexyl peaks same as for **10** with, δ_H 4.13 (s, 2H), 7.10 (s, 41H), 7.26 (m, 10H); GPC: M_n: 13 700, PDI: 1.2; MALDI-MS: m/z: 8002.1 [M$^+$] (calcd: 7997.6, DP of 47, benzyl/benzyl). Characterization of **7**: ^{1}H NMR (500 MHz, THF d_8): (Hexyl peaks same as for **10** with, δ_H 6.81 (d, J = 8.5 Hz, 4H), 7.07 (s, 34H), 7.28 (d, J = 8.5 Hz, 4H); GPC: M_n: 4118, PDI: 1.51; MALDI-MS: m/z: 4348.2 [M$^+$] (calcd: 4343.2, DP of 25, Ph-OH/Ph-OH). Characterization of **8**: ^{1}H NMR (500 MHz, $CDCl_3$): (Hexyl peaks same as for H/Br poly(3-hexylthiophene) with, δ_H 2.37 (s, 6H), 6.98 (s, 43H); GPC: M_n: 8.500, PDI: 1.1; MALDI-MS: m/z: 5185.9 [M$^+$] (calcd: 5184.8, DP of 31, methyl/methyl). Characterization of **9**: ^{1}H NMR (500 MHz, THF d_8): (Hexyl peaks same as for **10**, butyl peaks overlap with hexyl); GPC: M_n: 7506, PDI: 1.1; MALDI-MS: m/z: 4508.6 [M$^+$] (calcd: 4505.6, DP of 26, butyl/butyl).

Hierarchical Structure: Silicon Nanowires Standing on Silica Microwires**

By *Changhui Ye*,* *Lide Zhang*, *Xiaosheng Fang*, *Yinhai Wang*, *Peng Yan*, and *Jianwei Zhao*

Silicon nanowires are attractive building blocks for the next generation of nanoelectronic devices because they can function both as the core of the devices and as the interconnectors between components.[1] With the ongoing miniaturization of silicon-based electronics, conventional lithography is reaching its limits. Fortunately, the self-assembly of nanoscale building blocks has proven successful in microelectronics and this technique is accessible to many laboratories, since costly fabrication lines are avoided.[2] However, the fabrication of nanodevices by either a self-assembly or improved Langmuir–Blodgett approach still entails lengthy and elaborate processing, although the new, emerging, so-called hierarchical struc-

[*] Dr. C. Ye, Prof. L. Zhang, Dr. X. Fang, Prof. Y. Wang, Dr. P. Yan, Dr. J. Zhao
Key Laboratory of Materials Physics
Institute of Solid State Physics
Chinese Academy of Sciences
Hefei 230031 (P.R. China)
Email: chye@issp.ac.cn

[**] This work was supported by the Anhui Provincial Natural Science Foundation (Grant No. 03044905) and the National Science Foundation of China (Grant No. 10304018).

 DOI: 10.1002/adma.200306509

ADVANCED MATERIALS

tures may represent an alternative toward the scaling up of the building blocks into functional electronic devices. Ren's group has systematically explored the growth of hierarchical oxide structures, the core and branches of which display certain orientation relationships.[3] In contrast to the well-known dendritic structures, the core and the branches of the hierarchical structures can be built from different materials. Ren, Wang, and Zhu and their respective co-workers have demonstrated that various oxide semiconductors, such as ZnO, In_2O_3, or SiO_x hierarchical nanostructures, can be fabricated by simple evaporation and condensation processes, and they proposed that these novel structures could be applied in field emission, photovoltaics, supercapacitors, and so on.[4] However, Si is usually the core material for microelectronic devices, therefore hierarchical structures built directly from Si-based materials are expected to be an ideal research target towards the three-dimensional scaling-up of the building blocks as the basis for functional nanodevices.

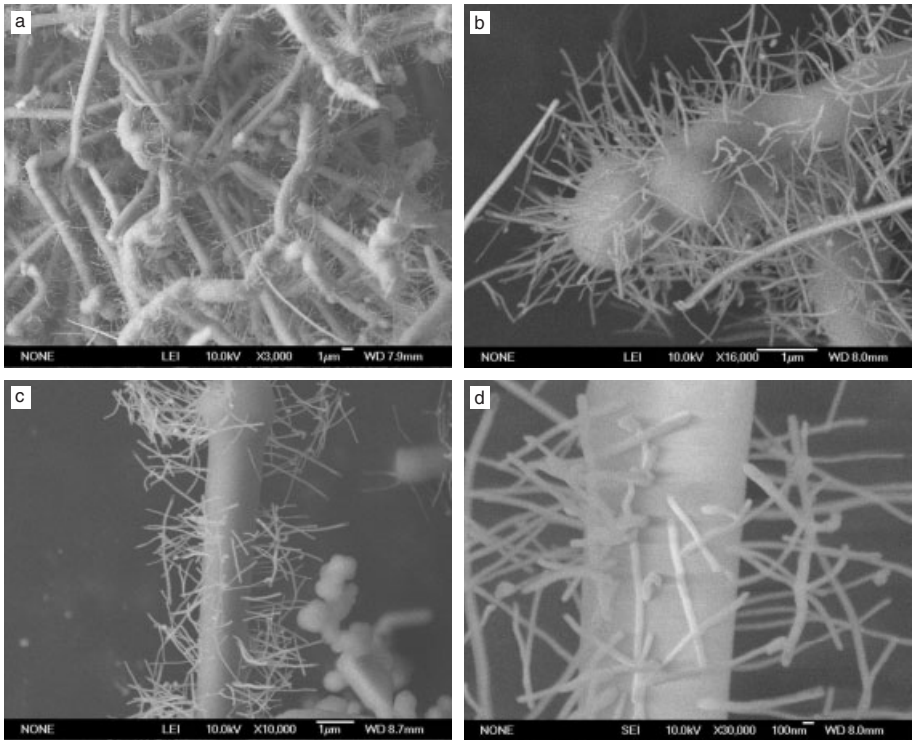

Figure 1. SEM images of the Si-based hierarchical structures. a) Low-magnification view of a large quantity of the hierarchical structures. b) High-magnification view of a typical hierarchical structure. c) A straight microwire with numerous nanowires erupting from it. d) Enlargement of the central section in (c).

In this communication, we report the fabrication of a novel hierarchical structure, namely single-crystalline Si nanowires standing on silica microwires. We adopt the disproportionation reaction of SiO ($2\,SiO \rightarrow SiO_2 + Si$) and are able to separate the deposition of SiO_2 and Si species into two steps to grow the hierarchical structures with metallic tin as a liquid-forming agent. This approach differs from the well-developed synthetic techniques for preparing Si or SiO_2 nanowires.[5]

Scanning electron microscopy (SEM) was employed to characterize the morphology of the as-synthesized product. The general morphologies of the hierarchical structures are displayed in Figure 1. A large quantity of microwires with numerous nanowires standing on them are shown in Figure 1a. A close-up view of the wires (Fig. 1b) reveals that many nanowires terminate with a spherical particle, which is typical of a vapor–liquid–solid (VLS) growth mechanism.[6] Figure 1c shows a straight microwire with many nanowires growing from it. The enlarged section of this image shown in Figure 1d indicates that these nanowires are grown-in from the microwire. The nanowires are straight and smooth with a typical length of several micrometers and a diameter ranging from 40 to 70 nm.

Transmission electron microscopy (TEM) observations allowed us to gain insight into further details of this structure. The nanowires could be broken off from the microwire by ultrasonic treatment in acetone solution. The low-magnification TEM image of a typical nanowire (Fig. 2a) reveals that the nanowire has a smooth surface with a particle at its tip. The high-resolution electron microscopy (HRTEM) image of this nanowire (Fig. 2b) shows the lattice fringes perpendicular to the wire axis. The spacing between the neighboring fringes is equal to 0.32 nm, which corresponds to the separation of the {111} lattice planes of Si. There is a thin amorphous layer on the nanowire, which may be SiO_x, in agreement with previous reports.[5] The electron diffraction (ED) pattern (inset in Fig. 2b) taken along the <110> zone axis agrees well with the HRTEM image and further indicates that the nanowire is a single crystal. The two spots in the ED pattern indexed as $(\bar{1}1\bar{1})$ and $(\bar{1}11)$indicate that these two lattice planes possess an inclination of 70.5°, which agrees with crystallography data of the cubic lattice of Si. This means that the nanowire grows along the $[\bar{1}1\bar{1}]$ direction. Energy-dispersive X-ray spectroscopy (EDX) reveals that this nanowire is composed of Si (Fig. 2c). The trace amount of oxygen observed may come from the amorphous SiO_x layer; Cu comes from the specimen holder. The particle at the tip of the nanowire consists of Sn, Si, and O (not shown here) and assists the growth of the Si nanowire.

The growth of the hierarchical structures can be divided into two consecutive steps. Upon decomposition of the SiO

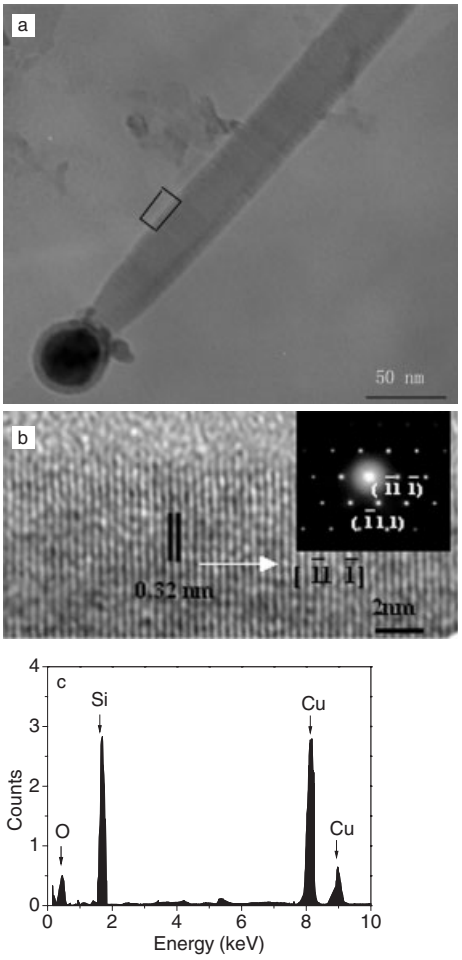

Figure 2. a) TEM image of a Si nanowire with a spherical nanoparticle at its tip. b) HRTEM image of the boxed section in (a). Inset is the corresponding ED pattern taken along the <110> zone axis. c) EDX pattern of this nanowire, where Si and a small amount of O are observed.

vapor to SiO_2 and Si, SiO_2 may grow rapidly as microwires or a nanoparticle aggregate. Si will form an alloy with Sn (formed by the decomposition of SnS nanoparticles) and will condense much slower than SiO_2 does owing to the low eutectic temperature of Si–Sn alloy (232.0 °C). Therefore, the deposition of the Si–Sn alloy on the surface of the SiO_2 microwires and subsequent VLS growth of Si nanowires from saturated Si–Sn alloys gives birth to the hierarchical structures. However, the deposition of the Si–Sn alloy on SiO_2 microwires is not necessarily uniform; consequently, some SiO_2 microwires grow without Si nanowires on them. Moreover, deposition of the Si–Sn alloy on the substrate may directly induce the Sn-assisted growth of Si nanowires, and this has indeed been observed in the SEM characterization. Figure 3a shows the growth of SiO_2 microwires and Si nanowires in close proximity. EDX analysis reveals that the microwires are indeed composed of Si and O with an atomic ratio close to 1:2 and that the nanowires composed of Si and a small amount of O (not shown).

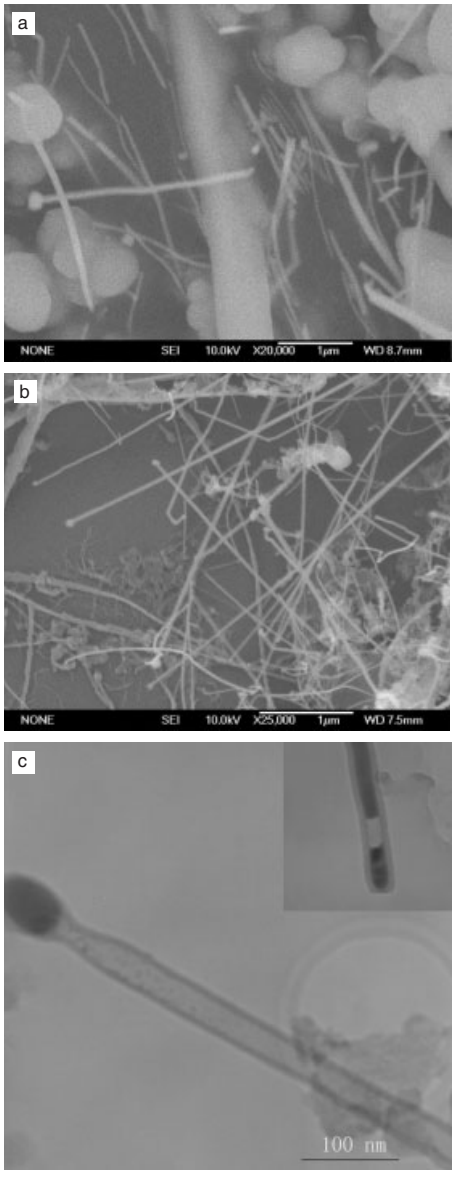

Figure 3. a) SEM image of the coexistence of SiO_2 microwires and Si nanowires. b) SEM image of the nanowires deposited on the substrate with Sn as the liquid-forming agent in the control experiment. c) TEM image of the by-product in the source region after the reaction in the regular experiment for the preparation of the hierarchical structure. The typical products therein are SiO_2 nanotubes and SiO_2 nanotubes partially filled with Sn (inset).

The questions still to be answered are: what is the determining factor for the two-step hierarchical assembly of Si nanowires on SiO_2 microwires; and why similar phenomena have not been reported by other researchers during the preparation of Si nanowires using the same precursor (SiO). We propose that the in situ alloying of Si and Sn to produce the liquid phase and transport to the substrate following the SiO_2 phase are most probably responsible for the formation of this particular structure. In a control experiment with micrometer-sized metallic Sn deposited directly on the substrate and pure SiO

ADVANCED MATERIALS

particles as the source material, only fine nanowires of Si and SiO_2 were produced, as displayed in Figure 3b. This may reveal the importance of the in situ alloying process and the separation of SiO_2 and Si species in the formation of the hierarchical structures. When trying to elucidate the operation of the two-step process, we analyzed the by-product left in the source region (originally containing SiO powder and SnS nanoparticles) in the regular experiment for the preparation of the hierarchical structure. Instead of the above-mentioned hierarchical structures, a distinct morphology was observed. The TEM image in Figure 3c represents a general structure of this morphology. It appears that Sn-assisted growth of silica nanotubes and silica nanotubes partially filled with Sn (inset in Fig. 3c) have been obtained, similar to the In-assisted silica and In-filled silica nanotubes reported recently by Li et al.[7] The above findings and the fact that simultaneous deposition of Si and SiO_2 usually gives SiO_2-sheathed Si nanowires explicitly indicates that a two-step process is responsible for the formation of the hierarchical structure. This is in agreement with the observations made by other researchers in growing oxide hierarchical structures, where a two-step process has also been proposed.[3,4]

As for the second step in the present study, the multiple nucleation of silicon nanowires on silica microwires from the initially deposited Sn–Si alloy particles supersaturated with Si followed by the supply of Sn–Si alloy in the gas phase is fully consistent with a VLS growth mechanism and the basal-growth aspects of the Si nanowires seen in the experiments.[6]

It is noteworthy that metals with a low melting temperature such as Ga (29.8 °C), In (156.6 °C), and Sn (231.9 °C) generally form alloys with Si at a low eutectic temperature rather close to the melting point of the respective metals. Furthermore, the atomic content of Si in the alloys at the eutectic temperature are as low as, or even lower than, one part per thousand. In particular, the solubility of Si in the alloy with Sn at the substrate temperature (500 °C) is 0.4 at.-%. The effectiveness of these metals in directing the growth of a wide variety of Si-based structures, first suggested by Sunkara et al.,[8] and confirmed by Pan et al.,[9] Li et al.,[7] and Sun et al.,[10] further suggests the importance of the nanometer-sized Sn liquid-forming agent for the derivation of the Si-based hierarchical structure in the present study.

The room-temperature photoluminescence (PL) spectrum of the hierarchical structures was measured at an excitation wavelength of 325 nm (Fig. 4). The emission spectrum reveals that the as-synthesized Si-based structure has a strong near-IR emission band centered at 910 nm and a weaker green one at 500 nm. The green emission band can be attributed to radiative recombination from the defect centers in the over-coated silicon oxide layer, such as oxygen vacancies, as suggested by Liao et al.[11] The near-IR emission band may possibly originate from defective Si nanowires, as proposed by Teo et al.[12]

In summary, novel hierarchical structures of single-crystalline Si nanowires standing on SiO_2 microwires have been synthesized by adopting Sn as the liquid-forming agent. The derivation of this kind of structure involves a two-step process, namely growth of SiO_2 microwires followed by deposition of Si and Sn alloys, which direct the growth of the Si nanowires. The intense near-IR PL suggests possible applications of the hierarchical structures in nanoscale optoelectronic devices. This facile scaling-up of the nanoscale building blocks of Si nanowires has implications in the fabrication of functional nanodevices such as optoelectronics and gas sensors.

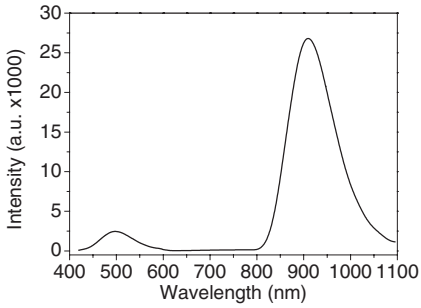

Figure 4. PL spectrum of the hierarchical structures, where a strong peak centered at 910 nm and a weak peak centered at 500 nm are observed.

Experimental

A horizontal ceramic tube (inner diameter 25 mm; length 80 cm) was mounted inside a tube furnace. SnS nanoparticles (0.5 g; average grain size ca. 60 nm) and analytical grade SiO powders (2 g, with diameter about 10 μm; purity greater than 99.99 %) were put in an alumina boat and then loaded into the central region of the ceramic tube. Then, a pre-cleaned Si wafer was placed at the downstream side of the source materials at a distance of 8 cm. After the tube had been purged with high-purity Ar for 30 min, the Ar flow-rate was set at 25 sccm. The temperature at the central region of the furnace was increased to 1200 °C in 10 min, and then maintained at this temperature for 2 h. The temperature at the substrate was close to 500 °C, as determined from the pre-measured temperature-gradient curve. After the furnace had cooled to room temperature, a dark gray wool-like product was deposited on the substrate. The collected products were characterized by scanning electron microscopy (SEM; JEOL JSM 6300), transmission electron microscopy (TEM; Hitachi 800 at 200 kV; HRTEM, JEOL 2010, at 200 kV), and energy-dispersive X-ray spectroscopy (EDX). The room-temperature photoluminescence (PL) spectrum was recorded with an Edinburgh luminescence spectrometer (FLS 920) using a xenon lamp (900) as the excitation source.

Received: November 23, 2003
Final version: February 18, 2004

[1] a) L. J. Lauhon, M. S. Gudiksen, D. Wang, C. M. Lieber, *Nature* **2002**, *420*, 57. b) Y. Cui, C. M. Lieber, *Science* **2001**, *291*, 851.
[2] a) P. Yang, *Nature* **2003**, *425*, 243. b) X. Duan, C. Niu, V. Sahi, J. Chen, J. W. Parce, S. Empedocles, J. L. Goldman, *Nature* **2003**, *425*, 274. c) A. Tao, F. Kim, C. Hess, J. Goldberger, R. He, Y. Sun, Y. Xia, P. Yang, *Nano Lett.* **2003**, *3*, 1229. d) D. Whang, S. Jin, Y. Wu, C. M. Lieber, *Nano Lett.* **2003**, *3*, 1255.
[3] J. Y. Lao, J. G. Wen, Z. F. Ren, *Nano Lett*. **2002**, *2*, 1287.
[4] a) J. Y. Lao, J. G. Wen, D. Z. Wang, Z. F. Ren, *Int. J. Nanosci*. **2002**, *2*, 149. b) J. Y. Lao, J. Y. Huang, D. Z. Wang, Z. F. Ren, *Nano Lett*. **2003**, *3*, 235. c) J. G. Wen, J. Y. Lao, D. Z. Wang, T. M. Kyaw, Y. L.

Foo, Z. F. Ren, *Chem. Phys. Lett.* **2003**, *372*, 717. d) Z. L. Wang, Z. W. Pan, *Adv. Mater.* **2002**, *14*, 1029. e) P. X. Gao, Z. L. Wang, *J. Phys. Chem. B* **2002**, *106*, 12653. f) P. X. Gao, Y. Ding, Z. L. Wang, *Nano Lett*. **2003**, *3*, 1315. g) Y. Q. Zhu, W. K. Hsu, M. Terrones, N. Grobert, H. Terrones, J. P. Hare, H. W. Kroto, D. R. M. Walton, *J. Mater. Chem.* **1998**, *8*, 1859. h) Y. Q. Zhu, W. K. Hsu, W. Z. Zhou, M. Terrones, H. W. Kroto, D. R. M. Walton, *Chem. Phys. Lett.* **2001**, *347*, 337.

[5] a) Y. F. Zhang, Y. H. Tang, N. Wang, D. P. Yu, C. S. Lee, I. Bello, S. T. Lee, *Appl. Phys. Lett.* **1998**, *72*, 1835. b) A. M. Morales, C. M. Lieber, *Science* **1998**, *279*, 208. c) N. Wang, Y. H. Tang, Y. F. Zhang, C. S. Lee, S. T. Lee, *Phys. Rev. B* **1998**, *58*, R16 024.

[6] R. S. Wagner, W. C. Ellis, *Appl. Phys. Lett.* **1964**, *4*, 65.

[7] Y. Li, Y. Bando, D. Golberg, *Adv. Mater.* **2004**, *16*, 37.

[8] a) M. K. Sunkara, S. Sharma, R. Miranda, G. Lian, E. C. Dickey, *Appl. Phys. Lett.* **2001**, *75*, 1546. b) S. Sharrma, M. K. Sunkara, *J. Am. Chem. Soc.* **2002**, *124*, 12 289. c) U. M. Graham, S. Sharma, M. K. Sunkara, B. H. Davis, *Adv. Funct. Mater.* **2003**, *13*, 576. d) S. Sharma, M. K. Sunkara, *Nanotech*. **2003**, *15*, 130. e) G. Bhimarasetti, M. K. Sunkara, U. M. Graham, B. H. Davis, C. Suh, K. Rajan, *Adv. Mater.* **2003**, *15*, 1629.

[9] a) Z. W. Pan, Z. R. Dai, C. Ma, Z. L. Wang, *J. Am. Chem. Soc.* **2002**, *124*, 1817. b) P. X. Gao, Y. Ding, Z. L. Wang, *Nano Lett*. **2003**, *3*, 1315. c) Z. W. Pan, S. Dai, D. B. Beach, D. H. Lowndes, *Appl. Phys. Lett.* **2003**, *83*, 3159. d) Z. W. Pan, S. Dai, D. B. Beach, D. H. Lowndes, *Nano Lett*. **2003**, *3*, 1279.

[10] S. H. Sun, G. W. Meng, M. G. Zhang, Y. T. Tian, T. Xie, L. D. Zhang, *Solid State Commun*. **2003**, *128*, 287.

[11] L. S. Liao, X. M. Bao, X. Q. Zheng, N. S. Li, N. B. Min, *Appl. Phys. Lett.* **1996**, *68*, 850.

[12] B. K. Teo, C. P. Li, X. H. Sun, N. B. Wong, S. T. Lee, *Inorg. Mater.* **2003**, *42*, 6723.

Micelle-Mediated Synthesis of Single-Crystalline Selenium Nanotubes**

By *Yurong Ma*, *Limin Qi*,* *Jiming Ma*, and *Humin Cheng*

Considerable attention has recently been directed towards one-dimensional (1D) nanostructures, such as wires, rods, belts, and tubes, owing to their unique physical and chemical properties and potential applications in nanoscale devices.[1] In particular, much effort has been devoted to the controlled synthesis of inorganic nanotubes since the discovery of carbon nanotubes.[2] A variety of inorganic nanotubes based on layered or pseudo-layered materials have been synthesized by using high-temperature or hydrothermal processes; examples include boron nitride, metal dichalcogenides, metal dihalides, metal oxides and hydroxides, metal borates, as well as metals.[3] Alternatively, nanotubes made from silica, alumina, silicon, and metals that do not possess a layered crystal structure have been fabricated by employing various templates such as porous membranes, carbon nanotubes, inorganic nanowires/nanorods, and organized assemblies of organic molecules,[4] however, these nanotubes are usually either amorphous or polycrystalline. Notably, there are a few reports of single-crystalline nanotubes composed of semiconductors with non-layered structures. Single-crystalline GaN[5] and Si[6] nanotubes have been produced by epitaxial overgrowth against suitable nanowire templates using vapor deposition processes. Interestingly, single-crystalline tellurium nanotubes have been obtained via a solution-phase approach, i.e., the polyol process where ethylene glycol refluxed at 197 °C served as both solvent and reducing reagent.[7] This soft solution processing strategy is promising but it still remains to be extended to inorganic materials other than tellurium. Therefore, it is a great challenge to develop new soft synthetic strategies that produce single-crystalline nanotubes from non-layered materials.

As an important elemental semiconductor, selenium shows many interesting properties, such as a relatively low melting point (~490 K), a high photoconductivity ($\sim 8 \times 10^4$ S cm^{-1}), nonlinear optical responses, and a high reactivity toward a variety of chemicals, and it finds commercial applications in photovoltaic cells, rectifiers, mechanical sensors, photographic exposure meters, and xerography.[8] Since the availability of 1D selenium nanostructures is expected to bring in new types of applications or to enhance the performance of the currently existing devices as a result of quantum-size effects, a number of synthetic methods have been developed to fabricate selenium nanorods and nanowires. Monoclinic selenium (m-Se) nanowires with a polycrystalline structure were obtained by using the protein cytochrome c_3 to reduce selenate (SeO_4^{2-}).[9] Xia et al. synthesized single-crystalline trigonal selenium (t-Se) nanowires via the reduction of selenious acid (H_2SeO_3) with excess hydrazine by solution refluxing[10] or sonochemical approaches.[11] Subsequently, t-Se nanowires and nanorods were produced by the dismutation of Na_2SeSO_3 under acidic condition[12] or the solution-mediated transformation from Se powders.[13] In addition, laser ablation and an evaporation and condensation process were used to prepare t-Se nanorods and nanowire networks, repectively.[14] It is noteworthy that Xia et al. have successfully synthesized a variety of novel 1D nanostructures including Ag_2Se nanowires, CdSe nanotubes, and Pt nanotubes by templating against the obtained Se nanowires.[15] However, to the best of our knowledge, there has been no report on the synthesis of uniform selenium nanotubes although large tubular single crystals of selenium were obtained under solvothermal conditions[16a] and irregular or broken selenium nanotubes were produced through a hydrothermal process followed by sonication.[16b] Here we describe a unique, facile, large-scale synthesis of single-crystalline t-Se nanotubes in micellar solutions of a

[*] Prof. L. Qi, Y. Ma, Prof. J. Ma, Prof. H. Cheng
State Key Laboratory for Structural Chemistry of Unstable and Stable Species, College of Chemistry, Peking University
Beijing 100871 (P.R. China)
E-mail: liminqi@chem.pku.edu.cn

[**] This work was supported by NSFC (20325312, 20233010), and the Special Fund of MOE, China (200020). Supporting Information is available from WileyInterscience or from the author.

DOI: 10.1002/adma.200400071